A Heuristic Method to Improve Power Cycling Related Lifetime in Series Connectable Modular Full-Bridge Inverter

DOI:
10.1109/EVER48776.2020.9243061

Document status and date:
Published: 12/09/2020

Document Version:
Accepted manuscript including changes made at the peer-review stage

A Heuristic Method to Improve Power Cycling Related Lifetime in Series Connectable Modular Full-Bridge Inverter

Juris Arrozy*, Henk Huisman, Jorge L. Duarte, and Elena A. Lomonova
Department of Electrical Engineering, Electromechanics and Power Electronics
Eindhoven University of Technology
Eindhoven 5612 AZ, The Netherlands
Email: j.arrozy@tue.nl

***Abstract*—This paper proposes a heuristic method to improve power cycling related lifetime in series connectable modular full-bridge inverters by means of load sharing. The load sharing scheme is realized by continuous alternation between two possible series configurations of the circuit at a heuristically-determined changeover frequency. Simulation results in the single-phase circuit are included, and the switches lifetime performance are compared with the reference cases. It is evident from the results that this method yields increased switches lifetime. Alternatively, it allows more current to be applied to the circuit for the same switches average junction temperature.**

***Keywords*—thermal swing, junction temperature, series connectable modular full-bridge inverter, losses, series configuration, changeover frequency.**

I. Introduction

In the recent years there has been growing interest in the development of electric vehicles. This includes the attention to the electric motor topologies development, namely dc motor, induction motor, permanent magnet synchronous motor, and synchronous reluctance motor [1]. Inseparable to the motor topologies are the power electronics circuits used for the drive system, which were also considered in [2] [3].

One of the major challenges in electric vehicle development is its reliability, especially in the power electronics circuit, since a malfunction in the power electronics device may prevent the vehicle to operate. Thus, several investigations have been done to assess the lifetime of semiconductor switches subjected to an electric vehicles mission-profile [4] [5]. It should be noted that the reliability and lifetime issue addressed throughout this paper is only concerned with the power cycling related failure and not the catastrophic failure.

The Coffin-Manson power cycle related lifetime model used in [6] indicates that the lifetime of the switch depends on its thermal swing and average junction temperature. The effect of the former is more apparent than the latter. Thus, several methods have been proposed to reduce the thermal swing of the switches. The first method uses active gate-driver as discussed in [7]. There, the gate voltage is adjusted to achieve near constant power losses independent of the current and this results in a thermal swing reduction. However, it yields a higher average junction temperature, therefore making the overall system less efficient. This method also requires a custom gate driver circuit, which will further complicate the implementation, especially in an inverter topology that has many switches. A different active gate-driving method discussed in [8] uses gate resistance variation to manipulate the switch losses, and in [9] combined with PWM frequency variation, which in turn produces less thermal swing. However, this method also requires a custom gate driver circuit implementation and influences the current ripple profile.

Another method also revolves around losses manipulation as it is directly correlated to the thermal swing profile. A commonly used method is switching frequency adjustment as was done in [10]. The idea is to decrease the switching frequency linearly based on the power increase. However the same problem occurs – thermal swing is reduced but the average junction temperature rises and the current ripple is varied. Therefore, in this paper a different approach is considered to achieve longer lifetime without increasing the average junction temperature.

The most straightforward method to reduce the average junction temperature is by means of load sharing. However, this is only possible in an inverter topology that meets a certain degree of redundancy, i.e. full redundancy in all phases. Unfortunately, this is not the case in most of the inverter topologies for electric drive application.

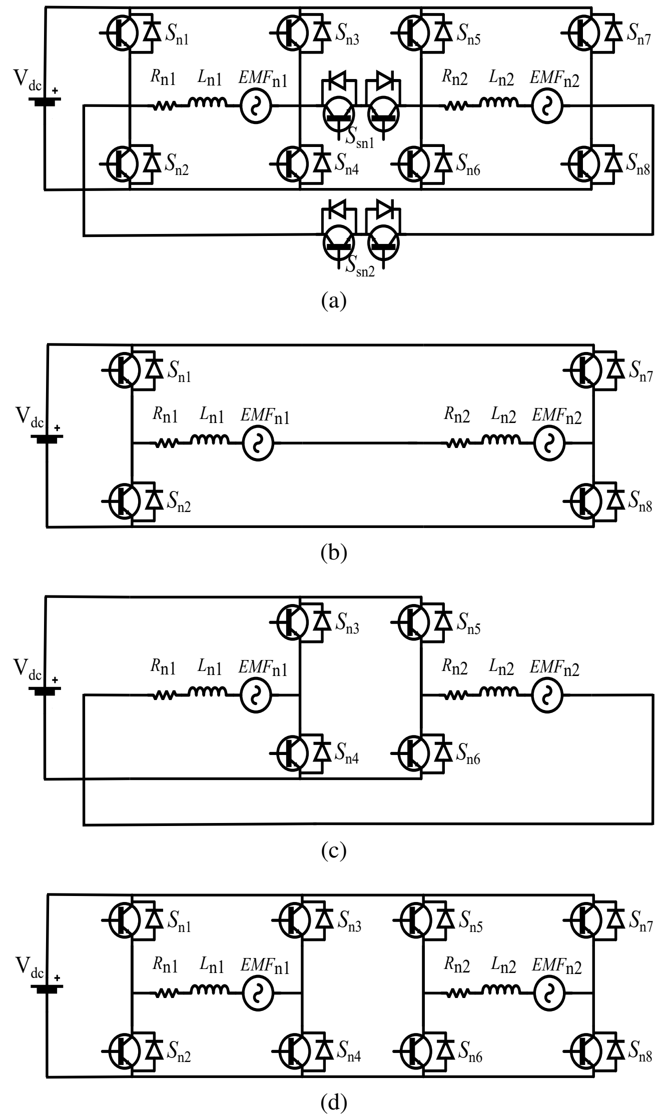

Figure 1: (a) Single-phase Series Connectable Modular Full-Bridge Inverter. (b) Series Configuration 1. (c) Series Configuration 2. (d) Independent Configuration

A review of fault-tolerant three-phase inverters for motor drive applications was included in [11]. In that review there is no inverter topology that meets the full redundancy requirement – single phase redundancy is the highest degree of redundancy that can be achieved.

The series connectable modular full-bridge inverter, first introduced in [12] and later elaborated more in [13] for driving a six-phase open-winding surface mounted permanent magnet synchronous motor [14], turned out to be able to be implemented with the load sharing scheme in order to reduce the average junction temperature. The windings can be connected either in series or driven independently by connecting/disconnecting the series switch in the circuit. In [15] the addition of an extra series switch and a new reconfiguration protocol between series and independent connection of the windings based on modulation index were proposed. The addition of an extra series switch results in the single-phase circuit of the series connectable modular full-bridge inverter as shown in Fig. 1a, where the index "n" denotes phase a, b, or c. Machine windings are modeled by resistance (R_{n1} and R_{n2}), inductance (L_{n1} and L_{n2}), and back EMF (EMF_{n1} and EMF_{n2}).

In Fig. 1, it is shown that for the series mode, two possible configurations exist. The first configuration is called series configuration 1 by using main switches S_{n1}, S_{n2}, S_{n7}, S_{n8}, and series switch S_{sn1} (Fig. 1b). The second configuration is called series configuration 2 by using main switches S_{n3}, S_{n4}, S_{n5}, S_{n6}, and series switch S_{sn2} (Fig. 1c). The changeover frequency between these two configurations can be optimized to reduce the main switches thermal swing, thereby increasing its lifetime performance.

This paper proposes a method of utilizing the circuit redundancy to achieve longer main switches lifetime. While alternation between the two series configurations is used to achieve a lower average junction temperature, its changeover frequency is optimized to reduce the thermal swing. The changeover frequency follows a linear relationship to the electrical frequency, which is obtained by using linear regression based on several sample points. This results in increased main switches lifetime or allows more current to be applied to the circuit for the same average junction temperature profile.

The remainder of this paper is organized as follows: section II describes the single-phase circuit of the series connectable modular full-bridge inverter and reviews the novel winding reconfiguration protocol introduced in [15] for clarity. In section III, the power losses and thermal model of the circuit are addressed. Section IV describes the lifetime model that is used to verify the effectiveness of the heuristic method proposed to achieve longer lifetime. Section V explains the heuristic method used to achieve reduced average junction temperature and thermal swing, which results in longer switches lifetime. Simulation results are included in section VI, providing the argument that not only the method will increase the lifetime of the switches, but alternatively it also allows more current to be applied to the circuit when the same average junction temperature is being considered. Drawbacks of the proposed method are also pointed out. Remarks on the changeover frequency determination in series-independent configuration are pointed out to further optimize the proposed heuristic method. Finally, in section VII the conclusion of the research and some remarks are addressed.

II. Single-Phase Series Connectable Modular Full-Bridge Inverter

Fig. 1a depicts the single-phase circuit of the series connectable modular full-bridge inverter investigated in this paper. The windings can be connected in series manner by utilizing the series configuration 1 switches group (Fig. 1b) or series configuration 2 switches group (Fig. 1c). When being operated in independent mode, the series switches are opened and all the eight main switches (S_{n1}-S_{n8}) are operated to drive the two windings independently from each other (Fig. 1d). It should be noted that the required modulation index to achieve a current value in independent mode is half of that of the series mode. By switching from series to independent mode the dc voltage can be utilized more, thus prolonging the constant torque operating region.

In previous work (see [13]), the winding reconfiguration protocol from series to independent and vice-versa was based on speed, where the modulation index in independent mode is half of that in the series mode (see Fig. 2). However, such a reconfiguration protocol will not be used for it introduces unnecessary switching losses. Instead, the reconfiguration protocol based on modulation index as in [15] is used.

Fig. 3 depicts the reconfiguration protocol based on modulation index. In this winding reconfiguration protocol, when the absolute value of modulation index exceeds one the windings are driven in independent mode and the modulation index intended for this mode is half of that in the series mode. After the absolute value of the original modulation index falls below 1 (0.5 in independent mode), the windings are reconnected in series manner and the original modulation index returns. This way, the independent mode utilization is reduced, thus reducing the switching loss. In the implementation, hysteresis is used to avoid chattering between series and independent mode. If the required speed/torque is low enough, the modulation index will be low and the circuit will be operated in all-time series mode, as shown in the left side of Fig. 3.

III. Losses and Thermal Model

Modeling the power losses of the switches is essential for predicting their lifetime. In the circuit used, the associated losses are divided into: (1) main switch conduction loss (p_{cond}); (2) series switch conduction loss ($p_{\text{cond,ss}}$); (3) main switch switching loss (p_{sw}). Those losses are formulated as follows:

$$p_{\text{cond}} = v_{\text{cond}} i_S \tag{1}$$

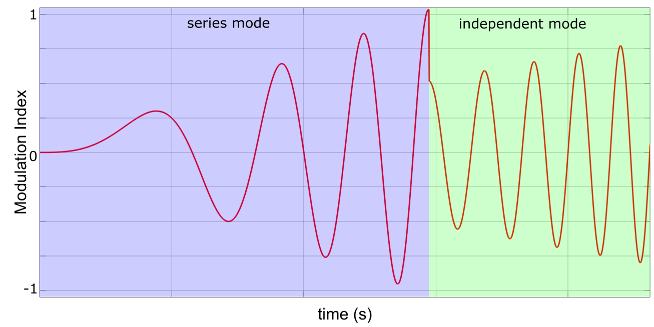

Figure 2: Winding Reconfiguration Based on Speed.

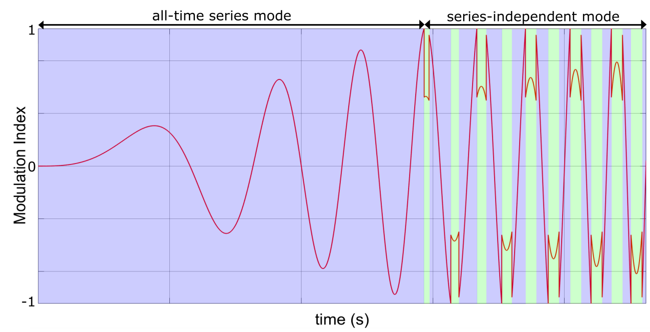

Figure 3: Winding Reconfiguration Based on Modulation Index (Independent Mode is Marked with Green Area).

$$p_{\text{cond,ss}} = v_{\text{cond,ss}} i_S + v_D i_S \tag{2}$$

$$p_{\text{sw}} = [E_{\text{on}}(i_S) + E_{\text{off}}(i_S) + E_{\text{rr}}(i_S)] f_{\text{s}} \tag{3}$$

where v_{cond} is the on-state voltage of the switch, v_D is the body diode on-state voltage, f_{s} is the switching frequency, and $E_{\text{on}}(i_S)$, $E_{\text{off}}(i_S)$, and $E_{\text{rr}}(i_S)$ are the turn-on energy loss, turn-off energy loss, and the body diode reverse recovery losses of the switch given the switch current i_S, respectively. Subscript ss is added when the series switch is being considered instead of the main switch.

However, as will be explained more thoroughly in section V, the heuristic method proposed in this paper includes alternation between two series configurations at a heuristically-determined changeover frequency (f_{ch}). The switching loss of the series switch that occurs during each changeover process ($p_{\text{sw,ss}}$) is formulated as

$$p_{\text{sw,ss}} = [E_{\text{on,ss}}(i_S) + E_{\text{off,ss}}(i_S) + E_{\text{rr,ss}}(i_S)] f_{\text{ch}} \tag{4}$$

and the switching loss of the main switch associated with each changeover ($p_{\text{sw,ch}}$) is formulated as

$$p_{\text{sw,ch}} = [E_{\text{on}}(i_S) + E_{\text{off}}(i_S) + E_{\text{rr}}(i_S)]f_{\text{ch}} \qquad (5)$$

Note that the expression in (4) and (5) only holds true in series mode. In independent mode, all the eight main switches are being operated while the series switches are left unused. Thus, no alternation can occur and consequently $p_{\text{sw,ss}}$ and $p_{\text{sw,ch}}$ are zero.

As for the thermal network, a three-ladder Foster network is used for the assumed ambient temperature of 25°C. The Foster networks RC parameters are shown in Table I, whereas the transient thermal impedance data of the switches used is depicted in Fig. 4.

i	$R_{\text{th}-i}$ (°C/W)	$C_{\text{th}-i}$ (J/°C)
1	0.0686	0.0139
2	0.0630	0.203
3	0.631	1.62

Table I: Foster Thermal Network Parameters of the Switch from [16].

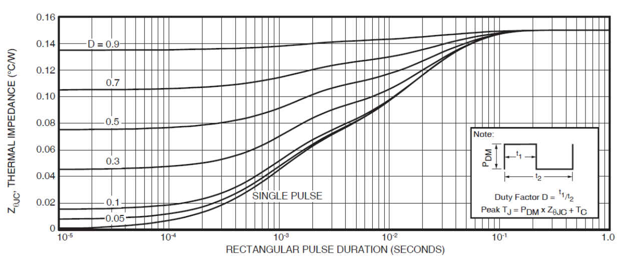

Figure 4: Transient Thermal Impedance Data of the Switch from [16].

In the simulation results, thermal interfacing material and heat sink thermal model are not taken into account. The reason is to clarify the effect of the proposed method to the lifetime of the switches without taking into account the contribution of the passive heat exchanger and to reach faster steady state junction temperature value. However, it should be clear that when such a method is applicable to a bare semiconductor switch, it will perform similarly in the environment where the switch is equipped with thermal interfacing material and heat sink.

IV. Switches Lifetime Model

The lifetime of the switch is mainly affected by thermal swing, average junction temperature, and constants related to the switch package. In this paper, the same constants as in [17] are used. From [6], the Coffin-Manson lifetime model is formulated as follows

$$N_{\text{f}} = A \cdot (\Delta T_{\text{J}})^{\alpha} \cdot \exp(\frac{E_a}{k_B \cdot T_{\text{J-avg}}}) \qquad (6)$$

where N_{f} is the number of cycles to failure of the switch, A is a fitting constant (650790 K), α is a fitting constant (-4.67), E_a is the activation energy (9.89 $\cdot 10^{-20}$ J), and k_B is the Boltzmann constant (1.38 $\cdot 10^{-23}$ J $\cdot$K^{-1}). It should be noted that although there are other lifetime models as reviewed in [18], the lifetime prediction resulted by the other models should be similar to the Coffin-Manson model.

From (6), the time to failure (t_{fail}), which indicates the lifetime of the switch, is calculated as follows

$$t_{\text{fail}} = \frac{N_{\text{f}}}{f_{\text{thermal}}} \qquad (7)$$

with f_{thermal} is the temperature cycle frequency.

The thermal swing of the switch is calculated as

$$\Delta T_{\text{J}} = P_{\text{loss}} Z_{\text{th}} \qquad (8)$$

where ΔT_{J} is the thermal swing of the switch, P_{loss} is the total loss of the switch, and Z_{th} is the transient thermal impedance of the switch (see Fig. 4 for an example).

V. Heuristic Method for Reduced Switches Average Junction Temperature and Thermal Swing

It is shown in (8) that ΔT_{J} is a function of P_{loss} and Z_{th}. The notion behind this method is to continuously alternate between two series configurations while the circuit is running in series mode, enabling the power cycle to be shared (thus reducing the p_{cond} and p_{sw} in a current cycle) and reducing the Z_{th} by decreasing the effective duty cycle.

It is seen from Fig. 5 that the modulation indexes applied to series configuration 1 and series configuration 2 switches group are the result of AND logic between the PWM signal (brown, Fig. 5) and the f_{ch} (green, Fig. 5). As the f_{ch} intensifies, the duty cycle applied to the main switches decreases. This results in a lower value of Z_{th}, as inferred from Fig. 4. It is seen that the changeover process might introduce a pulse signal with a small width. However, the signal width is still larger than the switching time of the switch plus the dead time

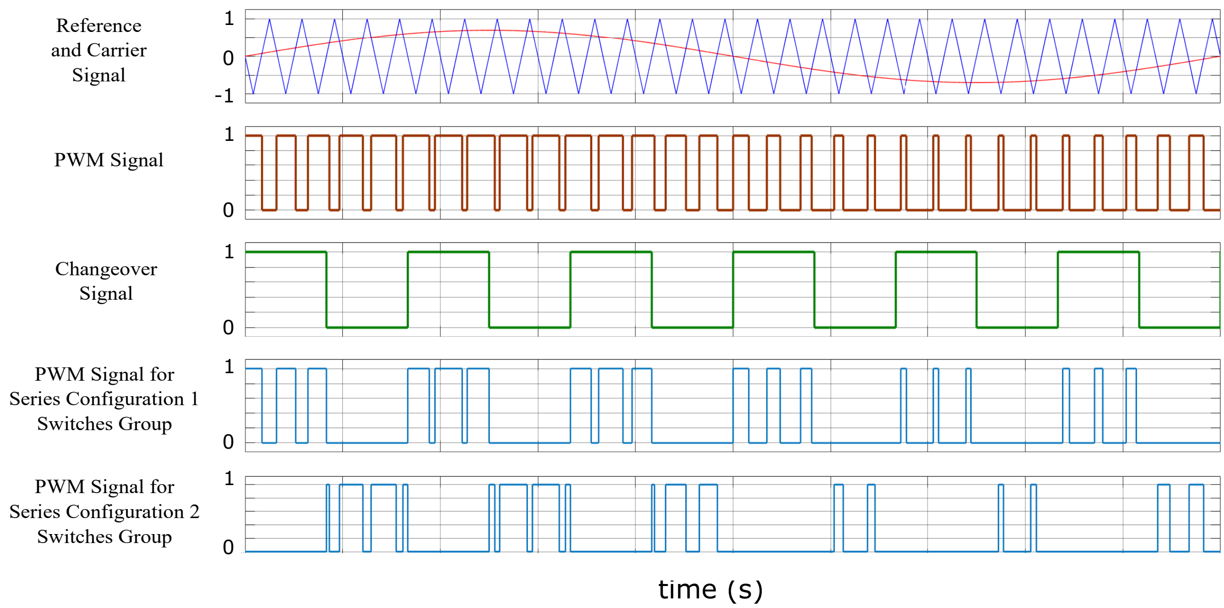

Figure 5: Example of Modulation Signal of the Switches Groups with Changeover.

implemented, as long as the changeover frequency is considerably lower than the carrier frequency.

However, careful consideration must be taken into account about the optimum f_{ch}, that is, changeover frequency which yields optimum lifetime performance as calculated from (6) and (7). A more frequent changeover indeed results in a lower Z_{th}, but it also produces more $p_{\text{sw,ch}}$ (see (5)) that adds to the total loss of the main switches. Moreover, in Fig. 4 it can also be seen that in relatively small rectangular pulse duration the Z_{th} value flattens. Thus, at one point increasing the f_{ch} will no longer necessarily result in a notable reduce of ΔT_{J}. In fact, because of the increasing $p_{\text{sw,ch}}$, the ΔT_{J} starts to rise.

Another issue to be addressed is that f_{ch} cannot exceed f_{s}, for it will highly distort the waveform generated due to the effect of dead time between each transition from one series configuration into another. In the circuit implementation, the selection of f_{ch} may also be affected by the parasitic inductance of the series switches connection (S_{sn1} and S_{sn2}), as high f_{ch} might introduce overvoltage during the series switch switching. However, in this paper the effect of parasitic inductance and dead time on the selection of the optimum f_{ch} is not addressed.

The optimum f_{ch} depends on the electrical frequency (f_{ac}). However, it is rather complicated to determine the optimum f_{ch} for every f_{ac} since it will be an optimization function of P_{loss}, Z_{th}, modulation index, and the current applied. Additionally, some of the parameters are intercorrelated with each other. For instance, E_{on} is a function of junction temperature, which in turn also affects the junction temperature. To avoid the complexity of computational effort with intercorrelated parameters, a heuristic method is proposed instead.

The heuristic method procedure is detailed as follows: first, one f_{ac} is run with several variations of f_{ch}. It is expected that as the f_{ch} increases, the ΔT_{J} decreases because of the shared stress and decreasing Z_{th} – thus increasing the N_{f} as in (6). However, as the f_{ch} further increases, the $p_{\text{sw,ch}}$ increases up to a point where it compensates the p_{cond} and p_{sw} decrease because of the load sharing while the Z_{th} flattens. This results in a higher ΔT_{J} and thus begins to shorten the main switches lifetime. The optimum f_{ch} is the one which results in optimum t_{fail} as calculated by using (7).

Second, the optimization procedure is executed for another f_{ac}. It is expected to have higher f_{ch} for higher f_{ac}. Finally, when enough data of f_{ac} and optimum f_{ch} is obtained, an approximated relationship between f_{ac} and f_{ch} is obtained by using linear regression.

Parameters	Value
Voltage (V)	320V
Current (A)	100A
Switching Frequency (f_s)	20kHz
Inductance	1mH
Resistance	0.1Ω

Table II: Circuit Parameters for the Single-phase Series Connectable Modular Full-Bridge Inverter.

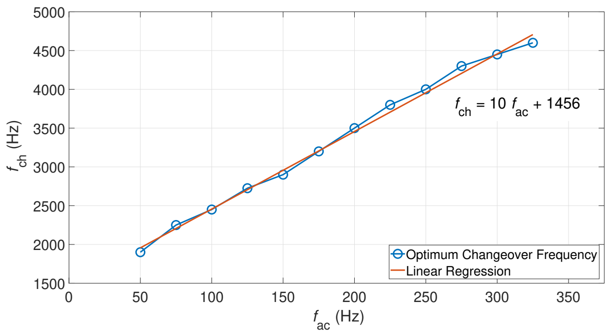

Figure 6: Electrical Frequency vs Optimum Changeover Frequency Plot.

Table II lists the inverter circuit parameters used as a test bench, while the resulting relationship between f_{ac} and optimum f_{ch} is depicted in Fig. 6. It is to be noted that 100A is chosen as the reference case to obtain a prominent effect on the temperature profile. However, it should be clear that the method also works for lower currents. From several test points, the relationship between f_{ch} and f_{ac} is estimated as f_{ch}=10f_{ac}+1456.

The heuristically-determined relationship between f_{ch} and f_{ac} from Fig. 6 is used for the rest of this paper. Comparison with the reference cases, that is, no changeover and changeover after a full current cycle, is highlighted to see the effect of the method on switches lifetime performance.

VI. Simulation Results

A. Remarks on All-time Series Mode

Table III and Fig. 7 show the comparison of the main and series switches temperature profile when:

- only one series configuration is used in the series mode (no changeover),
- changeover from series configuration 1 to series configuration 2 and vice versa occurs after a full current cycle,
- changeover based on the heuristic relationship between f_{ac} and f_{ch}.

It is to be noted that in this subsection all of the simulations are done in all-time series mode.

It is shown that the full-cycle method provides better $T_{\text{J-avg}}$ value than the no changeover method. It is because in full-cycle method, the current stress is shared between two switches groups thus reducing the $T_{\text{J-avg}}$. However, the ΔT_{J} rises because in the period of one switches group inactivity after a full current cycle, the switches temperature starts to drop before being reactivated in the next cycle.

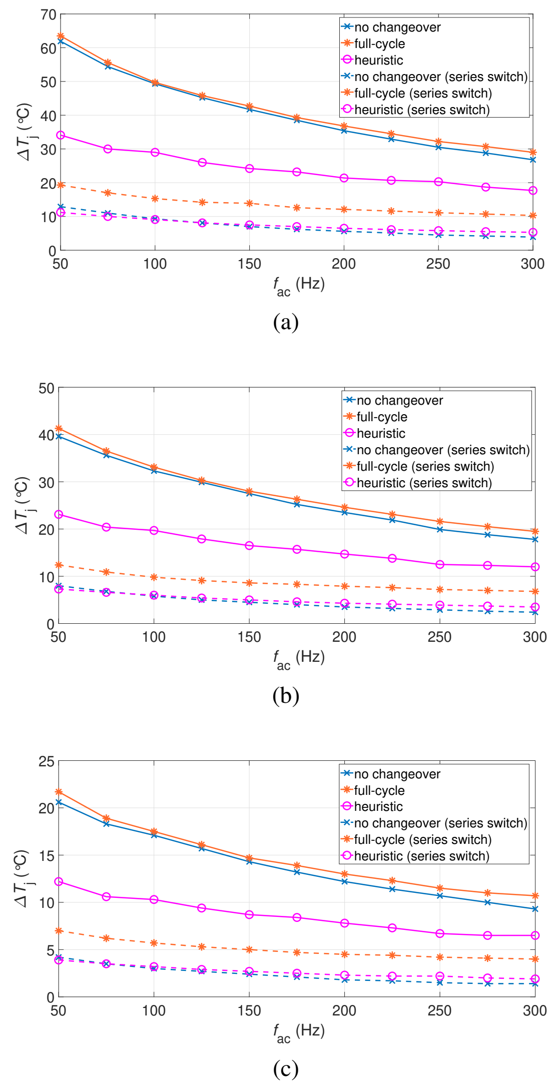

Figure 7: Thermal Swing Profile of the Main and Series Switches when (a) I=100A (b) I=75A (c) I=50A.

I (A)	no changeover		full-cycle		heuristic	
	$T_{\text{J-avg}}$	$T_{\text{J-avg,ss}}$	$T_{\text{J-avg}}$	$T_{\text{J-avg,ss}}$	$T_{\text{J-avg}}$	$T_{\text{J-avg,ss}}$
100	55	42	40	34	42	44
75	46	36	36	31	37	38
50	36	32	31	28	32	32

Table III: Average Junction Temperature of the Main and Series Switches (Temperature Results are Shown in °C).

The heuristic method turns out to be able to provide less ΔT_{J} and reduced $T_{\text{J-avg}}$ compared to the no changeover method because of the shared p_{cond}, p_{sw}, and decreased Z_{th}. A slight increase in $T_{\text{J-avg}}$ compared to the full-cycle method is expected because of the effect

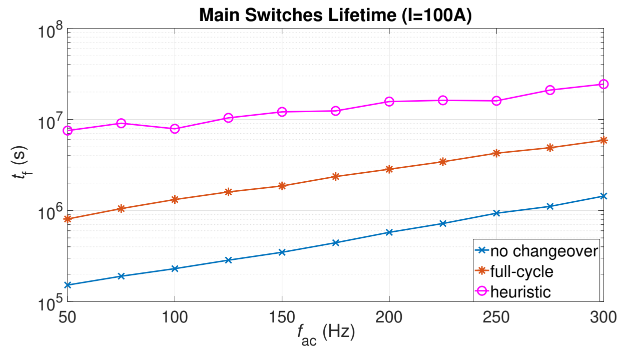

(a)

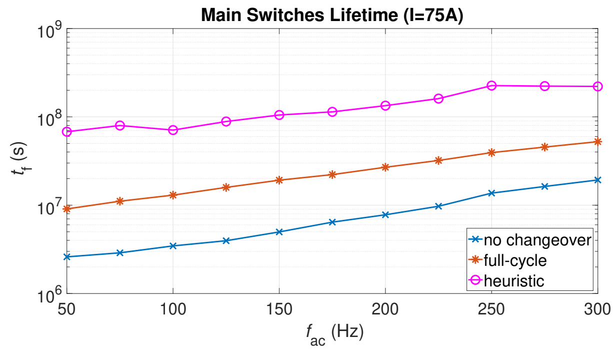

(b)

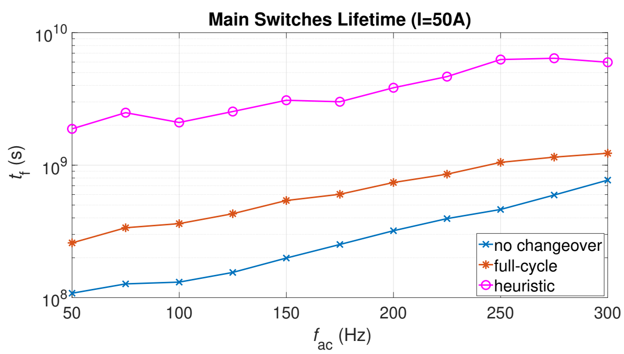

(c)

Figure 8: Main Switches Lifetime for (a) I=100A (b) I=75A (c) I=50A.

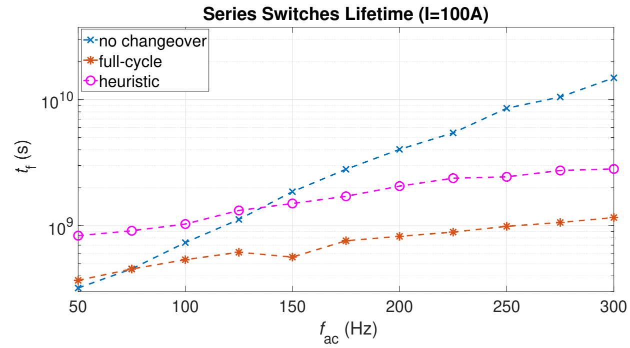

(a)

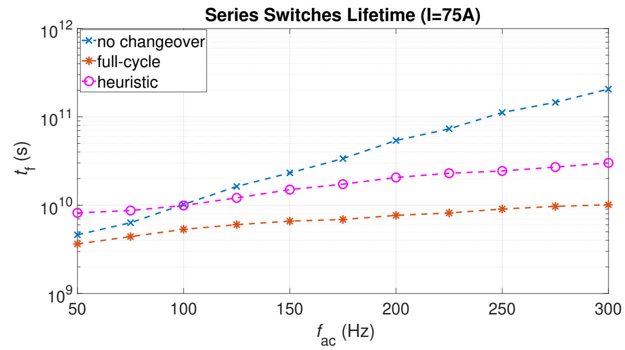

(b)

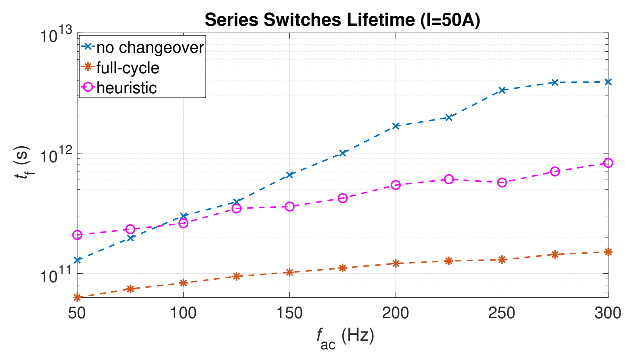

(c)

Figure 9: Series Switches Lifetime for (a) I=100A (b) I=75A (c) I=50A.

of $p_{\text{sw,ch}}$. A more apparent effect of f_{ch} on the $T_{\text{J-avg}}$ occurs in the series switches. This is because in the no changeover method no $p_{\text{sw,ss}}$ occurs and in the full-cycle method the f_{ch} is half of the f_{ac}, which yields a very low $p_{\text{sw,ss}}$. A steep increase of f_{ch} in the heuristic method introduces extra $p_{\text{sw,ss}}$ in the series switches which increases the $T_{\text{J-avg}}$.

By using (6) and (7) and the switches thermal performance from Table III and Fig. 7, the lifetime performance of the switches is predicted, as seen in Fig. 8 (main switches) and Fig. 9 (series switches). It is evident from Fig. 8 that by using the heuristic method, the main switches lifetime increases by a factor of >10 in all cases. This proves the effectiveness of the method to increase the main switches lifetime performance.

The reader should be aware of the effect of heuristic method on the lifetime of the series switches, as seen in Fig. 9. As the f_{ac} increases, the difference between the series switches f_{ch} of the no changeover and heuristic method also increases. This introduces extra $p_{\text{sw,ss}}$ (see (4)), which in turn affects its lifetime. In this paper, the size of the series switches and the main switches are identical. Therefore, the overall lifetime of the series switches are still longer than the main switches because the thermal stress on the series switches is less than that of the main switches. However, if the thermal performance of the series switches were to be degraded for economical reason, the effect of the heuristic method on the lifetime of the degraded series switches and its lifetime comparison to the lifetime of the main switches must be considered.

As seen in Table III, the heuristic method turns out to be able to reduce the $T_{\text{J-avg}}$ compared to the no changeover method. While in one way it means that the lifetime of the switches is increased, it also means that for the same average junction temperature profile more current can be applied to the circuit. This is seen in Table IV:

Current (A)	$T_{\text{J-avg}}$, no changeover (°C)	$T_{\text{J-avg}}$, heuristic (°C)
100	55	42
133	74	55

Table IV: Average Junction Temperature of the Main Switches (f_{ac}=300Hz).

For f_{ac}=300Hz, it is seen that the heuristic method allows the main switches to achieve 33% higher current with the same $T_{\text{J-avg}}$. This is crucial in electric vehicle application because it means that more torque can be applied to the motor without exceeding the junction temperature limit of the switches.

B. Remarks on Series-Independent Mode

In the independent mode, all the main switches are operated and the series switches are left idle. This means that in the independent mode no changeover can occur. As the required modulation index goes higher, the independent mode duration is prolonged. Thus, there is less available space for the changeover scheme.

The series-independent mode raises a question as to whether the f_{ch} should continue to follow the linear relationship to f_{ac} (knowing that as the f_{ac} grows there will be less space for changeover) or hold the f_{ch} constant at f_{ac} equals to the highest frequency achieved in all-time series mode. In the simulation, the series-independent mode begins approximately at f_{ac}=350Hz. Thus, the f_{ch} is held constant at f_{ac} below 350Hz. f_{ac}=325Hz is chosen in this case, resulting in constant f_{ch} of 4706Hz.

Fig. 10 depicts the main switches lifetime performance when a linear relationship between f_{ac} and f_{ch} is being maintained (red line) and when the f_{ch} is being held constant at 4706Hz after f_{ac} reaches 350Hz (blue line). It is seen that when the f_{ch} is held constant in the series-independent mode, it provides a longer main switches lifetime performance compared to when

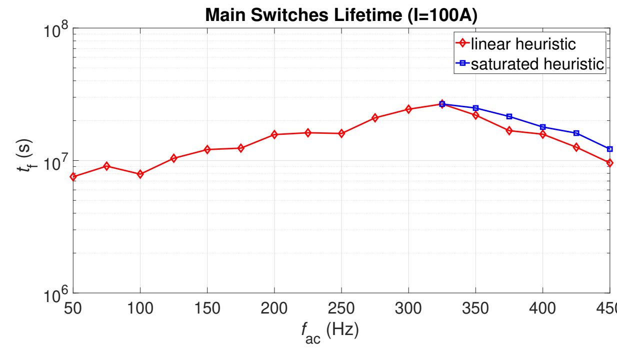

Figure 10: Main Switches Lifetime in Series-Independent Mode.

the linear relationship is being maintained in series-independent mode. This is because in series-independent mode, as stated previously, the series mode duration is shorter because of the introduction of independent mode. This provides less space for the heuristic method to optimize by constant alternation between two series configurations. Another point to be highlighted is that the f_{ch} rises (which results in higher $p_{\text{sw,ch}}$) while the Z_{th} does not decrease significantly because of the shorter series configuration duration.

Thus, in series-independent mode, it is more preferable to hold the f_{ch} constant. It is pertinent to know in which f_{ac} the series-independent mode begins. This allows one to keep in mind up to which point the linear relationship between f_{ac} and f_{ch} should be maintained.

VII. Conclusion

This paper proposes a heuristic method to reduce both the thermal swing and average junction temperature in a series connectable modular full-bridge inverter. The results show that the proposed method leads to a longer lifetime of the main switches. However, the method also shortens the lifetime of the series switches because of the switching losses resulting from the relatively high changeover frequency compared to the electrical frequency. Because of the reduced average junction temperature, the main switches can be subjected to more current for the same value of average junction temperature. A 33% increase in current is indicated by the simulation results. In series-independent mode it is shown that keeping the changeover frequency constant is preferable rather than following the linear regression pattern, due to the method is no longer as effective as it was in all-time series mode.

Acknowledgment

This paper is part of the ModulED *project that has received funding from the* European Union's Horizon 2020 research and innovation programme *under grant agreement No 79953*.

The author also wishes to thank Jigme Gurung for the discussions during the completion of his thesis work, which partly inspire the development of the method reported in this paper.

References

[1] J. de Santiago, H. Bernhoff, B. Ekergård, S. Eriksson, S. Ferhatovic, R. Waters, and M. Leijon, "Electrical motor drivelines in commercial all-electric vehicles: A review," *IEEE Transactions on Vehicular Technology*, vol. 61, no. 2, pp. 475–484, Feb 2012.

[2] B. A. Welchko and J. M. Nagashima, "The influence of topology selection on the design of EV/HEV propulsion systems," *IEEE Power Electronics Letters*, vol. 1, no. 2, pp. 36–40, June 2003.

[3] Z. Q. Zhu and D. Howe, "Electrical machines and drives for electric, hybrid, and fuel cell vehicles," *Proceedings of the IEEE*, vol. 95, no. 4, pp. 746–765, April 2007.

[4] D. Hirschmann, D. Tissen, S. Schröder, and R. W. De Doncker, "Reliability prediction for inverters in hybrid electrical vehicles," *IEEE Transactions on Power Electronics*, vol. 22, no. 6, pp. 2511–2517, Nov 2007.

[5] Z. Qiu, J. Zhang, P. Ning, and X. Wen, "Lifetime evaluation of inverter IGBT modules for electric vehicles mission-profile," in *2016 19th International Conference on Electrical Machines and Systems (ICEMS)*, Nov 2016, pp. 1–5.

[6] R. Amro, J. Lutz, and A. Lindemann, "Power cycling with high temperature swing of discrete components based on different technologies," in *2004 IEEE 35th Annual Power Electronics Specialists Conference (IEEE Cat. No.04CH37551)*, vol. 4, June 2004, pp. 2593–2598 Vol.4.

[7] L. Wang, B. Vermulst, and J. Duarte, "Thermal stress reduction and lifetime improvement of power switches with dynamic gate driving strategy," in *EPE'19 ECCE Europe*, 8 2019.

[8] C. H. van der Broeck, L. A. Ruppert, R. D. Lorenz, and R. W. De Doncker, "Active thermal cycle reduction of power modules via gate resistance manipulation," in *2018 IEEE Applied Power Electronics Conference and Exposition (APEC)*, March 2018, pp. 3074–3082.

[9] ——, "Methodology for active thermal cycle reduction of power electronic modules," *IEEE Transactions on Power Electronics*, vol. 34, no. 8, pp. 8213–8229, Aug 2019.

[10] M. Andresen, G. Buticchi, J. Falck, M. Liserre, and O. Muehlfeld, "Active thermal management for a single-phase H-bridge inverter employing switching frequency control," in *Proceedings of PCIM Europe 2015; International Exhibition and Conference for Power Electronics, Intelligent Motion, Renewable Energy and Energy Management*, May 2015, pp. 1–8.

[11] B. A. Welchko, T. A. Lipo, T. M. Jahns, and S. E. Schulz, "Fault tolerant three-phase ac motor drive topologies: a comparison of features, cost, and limitations," *IEEE Transactions on Power Electronics*, vol. 19, no. 4, pp. 1108–1116, July 2004.

[12] T. Gerrits, C. G. E. Wijnands, J. J. H. Paulides, and J. L. Duarte, "Electrical gearbox equivalent by means of dynamic machine operation," in *Proceedings of the 2011 14th European Conference on Power Electronics and Applications*, Aug 2011, pp. 1–10.

[13] ——, "Fault-tolerant operation of a fully electric gearbox equivalent," *IEEE Transactions on Industry Applications*, vol. 48, no. 6, pp. 1855–1865, Nov 2012.

[14] T. Gerrits, J. L. Duarte, C. G. E. Wijnands, E. A. Lomonova, J. J. H. Paulides, and L. Encica, "Twelve-phase open-winding spmsm development for speed dependent reconfigurable traction drive," in *2015 Tenth International Conference on Ecological Vehicles and Renewable Energies (EVER)*, March 2015, pp. 1–7.

[15] B. Daniels, J. Gurung, H. Huisman, and E. Lomonova, "Feasibility study of multi-phase machine winding reconfiguration for fully electric vehicles," in *2019 Fourteenth International Conference on Ecological Vehicles and Renewable Energies (EVER)*, 5 2019.

[16] Microsemi Corporation, "Advanced power technology," APT75GN120B2G datasheet.

[17] N. H. Baars, C. G. E. Wijnands, and J. L. Duarte, "Reduction of thermal cycling to increase the lifetime of MOSFET motor drives," in *IECON 2014 - 40th Annual Conference of the IEEE Industrial Electronics Society*, Oct 2014, pp. 1740–1746.

[18] C. Busca, "Modeling lifetime of high power igbts in wind power applications - an overview," in *2011 IEEE International Symposium on Industrial Electronics*, June 2011, pp. 1408–1413.